Biomass and Bioenergy 107 (2017) 113–121

Contents lists available at ScienceDirect

Biomass and Bioenergy

journal homepage: http://www.elsevier.com/locate/biombioe

Research paper

Thermophysical properties of rapeseed oil methyl esters (RME) at high pressures and various temperatures evaluated by ultrasonic methods

P. Kiełczyński [a, *], S. Ptasznik [b], M. Szalewski [a], A. Balcerzak [a], K. Wieja [a], A.J. Rostocki [c]

[a] Institute of Fundamental Technological Research, Polish Academy of Sciences, ul. Pawińskiego 5B, 02-106 Warsaw, Poland
[b] Department of Fat and Meat Technology, Institute of Agricultural and Food Biotechnology, ul. Jubilerska 4, 04-190 Warsaw, Poland
[c] Faculty of Physics, Warsaw University of Technology, ul. Koszykowa 75, 00-662 Warsaw, Poland

ARTICLE INFO

Article history:
Received 9 December 2016
Received in revised form
21 September 2017
Accepted 22 September 2017

Keywords:
Biofuels
Methyl esters
Phase transitions
Viscosity
Speed of sound
Ultrasonic methods
High pressure

ABSTRACT

Investigation of the high-pressure thermophysical properties of biofuels, e.g., bulk modulus, surface tension, and viscosity is of paramount importance in fuel injection systems in diesel engines. Another crucial and dangerous phenomenon that may occur in biofuels at high pressures is phase transition (solidification), which can drastically increase the viscosity of the biofuel. This effect may hamper proper operation of the engine, especially under cold-start conditions. Unfortunately, the availability of high-pressure thermophysical properties of biofuels is still limited. The goal of this paper is to investigate the impact of high pressures on thermophysical properties of biofuels on the example of rapeseed fatty acid methyl esters (RME) in a wide range of pressures (0.1 *to* 250 *MPa*) and temperatures (5 *to* 20 $^{\circ}C$). To this end we employed innovative ultrasonic techniques, i.e., the Bleustein-Gulyaev surface acoustic waves for measuring RME viscosity, and ultrasonic bulk compressional waves for measuring sound velocity in RME and consequently evaluating RME thermophysical parameters, e.g., bulk modulus and surface tension. The viscosity of the measured RME displayed an abrupt increase at pressures: 260 MPa ($t = 20\,^{\circ}C$), 230 MPa ($t = 15\,^{\circ}C$), 190 MPa ($t = 10\,^{\circ}C$), and 130 MPa ($t = 5\,^{\circ}C$). Evidently it was a signature of the phase transition (solidification) occurring in the RME. The discovered high viscosity high-pressure phase in RME can be very detrimental for operation of modern common rail Diesel engines. Therefore, the results of research presented in this paper should be interesting for engineers and designers working with modern common rail Diesel engines using biofuels.

1. Introduction

Application of high pressures in fuel injection systems for diesel engines is one of the possible ways to improve combustion efficiency and reduce harmful gas emission. Increased pressures have many advantages such as: better atomization of fuels and improved corresponding characteristics. On the other hand, new fuel injection systems (common rail) are inherent high-pressure systems. Therefore, the optimization of operation of common rail injection systems requires in depth understanding and knowledge of thermophysical parameters of biofuels and their components in a wide range of pressure, what consequently is of crucial importance for designers of common rail injection systems. The thermophysical parameters of biofuels that significantly affect the injection process are as follows: viscosity, density, bulk modulus and surface tension [1].

1.1. High-pressure phase transitions (solidification) in RME

One of the major challenges in the use of biofuels at high pressures is a possibility of occurrence of high-pressure phase transitions i.e., transformation of liquid fuel into a solid-like medium (solidification). In fact, an inherent feature of modern fuel injection systems (e.g., common rail) for diesel engines is the presence of a reservoir (common rail) that contains fuel at very high pressure values (up to 300 MPa). At pressures over 200 MPa a phase transition (solidification) may occur in biofuels. This solidification can result in significant problems of engine failure under cold-start conditions. The resulting new high-pressure phase is characterized by high viscosity and increased density.

Biofuels used in diesel engines, consist mainly of methyl and ethyl esters of fatty acids [2–7]. Rapeseed fatty acid methyl esters

* Corresponding author.
E-mail address: pkielczy@ippt.gov.pl (P. Kiełczyński).

https://doi.org/10.1016/j.biombioe.2017.09.015
0961-9534/

(RME) are the most commonly used additive for biofuels in moderate climate zone. Therefore, rapeseed oil methyl esters (RME), were selected for investigation in this paper.

This solidification process can be important in the low temperature range (below 20 °C). This fact can justify the choice of the temperature range in which investigations of the RME's properties have been performed by the authors.

The existence of these high-pressure phase transitions in biofuels has not been yet systematically studied and documented. For example, in paper [8] a phase transition in RME was detected qualitatively using an optical method. A rapid decrease of the RME sample transparency was attributed to a phase transition occurring in the measured RME sample.

By contrast, in the present paper, the Authors investigate high-pressure phase transitions in RME quantitatively, using an innovative ultrasonic technique. To this end, viscosity isotherms of the RME sample were measured, using surface acoustic waves of the Bleustein-Gulyaev (B-G) type. The measurements were performed as a function of pressure from 0.1 up to 350 MPa. Discontinuity and the following abrupt increase of the viscosity versus pressure was a clear indication that a high-pressure phase transition occurred in the measured RME sample. We stated the presence of high-pressure phase transitions of the first order in RME (FAME).

1.2. High-pressure thermophysical properties of RME

The thermophysical properties of biofuels are required for the efficient design of every step in their production, distribution, and utilization [9]. Knowledge of high-pressure thermophysical parameters, such as bulk modulus B, density ρ, viscosity η, and surface tension σ, of these liquids (RME) allows for prediction of their performance characteristics, e.g., parameters of atomization and combustion of the corresponding biofuels [10]. It has been shown in paper [11] that a suitable biodiesel fuel in a Direct Injection (DI) engine requires carefully balanced values of viscosity η, density ρ, bulk modulus B and surface tension σ, for a given atomizer to operate properly. Proper atomization enhances the mixing and complete combustion in a direct injection engine (DI), and hence is an important factor in engine emission and performance [11].

Unfortunately, so far in the literature of the matter, there is an insufficient data on the thermophysical properties of biofuels and their components (e.g., methyl esters) at high pressure conditions and at various temperatures [9,12–14].

The fundamental goal of this paper is twofold. Firstly, we investigate the possibility of occurrence of high-pressure phase transitions (solidification) in biofuels. Secondly, we investigate the impact of high pressures and temperatures on thermo-physical properties of biofuels. Investigations were performed on the example of rapeseed oil fatty acid methyl esters (RME), which are typical components of biofuels [6,7]. The corresponding measurements were performed using innovative ultrasonic techniques at pressures from 0.1 to 500 MPa and temperatures from 5 to 20 °C.

It is noteworthy that traditional measurements of thermophysical parameters of liquids (biofuels) at high-pressure range using conventional methods (e.g., the measurement of the surface tension σ by the Wilhelmy plate method, the capillary rise method, and the drop weight method) are very difficult, coarse and even impossible to be performed.

To overcome disadvantages of the conventional methods, the authors applied the original ultrasonic techniques [15] to evaluate the high-pressure thermophysical parameters of RME. For example, the viscosity η of liquids at high pressures was measured with SH (Shear Horizontal) surface acoustic waves of the Love and Bleustein-Gulyaev (B-G) type, propagating in solid waveguides immersed in the measured liquid. This measurement method have been originally proposed and developed by the Authors at the Institute of Fundamental Technological Research in Warsaw [16,17]. On the other hand, the speed of sound c (pressure waves) in liquids was determined from measurements of the time-of-flight (TOF) of bulk compressional (longitudinal) ultrasonic waves propagating in the measured liquid between two immersed ultrasonic transducers.

Availability of thermophysical parameters of biofuels such as density, viscosity, bulk modulus, and surface tension is of fundamental importance for practitioners (designers) in determining the optimum parameters of the processes of injection, atomization, ignition, and combustion of fuels in engines [9].

The speed of sound c (pressure waves) and viscosity η of the RME sample was measured ultrasonically, as a function of pressure p for various values of temperature T. The results of measurements for the speed of sound c and density ρ, as a function of pressure p and temperature T, were approximated by analytical formulas, i.e., third and fifth order polynomials of two independent variables p and T. From the measured speed of sound c (pressure waves) and density ρ, other crucial high-pressure thermophysical parameters of the investigated RME sample, such as its bulk modulus B, surface tension σ, etc., were evaluated using appropriate analytical formulas.

The results of measurements and mathematical modelling presented in this paper, for example the discovery of high-pressure phase transitions (solidification) in the fuel, can be of paramount importance for researchers working on fundamental problems e.g., mathematical simulation of thermophysical properties of biofuels. In addition, the results presented in this paper can be of particular significance for engineers and designers occupied with numerical modelling, design and optimization of new modern fuel injection systems (common rail) in diesel engines.

The results of research outlined in this work may also raise awareness of potential pitfalls (e.g., solidification) that may occur when designing new injection systems (common rail) with RME based biofuels.

2. Materials and methods

2.1. Properties of the measured RME

Measurements were performed for samples of the rapeseed fatty acid methyl ester (RME). Fatty acids methyl esters of rapeseed oil are obtained by transesterification of triacylglycerols using methanol (CH_3OH). Transesterification involves the exchange of chemically bound glycerol in the triacylglycerol (TAG) molecule to the added methyl alcohol in the presence of an alkaline catalyst. The catalyst for the reaction are the alkoxide ions. In our case, the transesterification process was catalyzed by sodium methoxide (CH_3ONa). As a result of this reaction, we obtain a mixture of methyl esters of fatty acids (RME) and a glycerol fraction which also contains sodium soaps and other unreacted products. After the transesterification process, RME samples were purified from these remains and distilled.

The transesterification process and analysis (by gas chromatography method) of the chemical composition of the obtained RME were carried out at the Laboratory in the Institute of Agricultural and Food Biotechnology in Warsaw, Poland.

Raw material (rapeseed oil) used to fabricate the RME was provided by the Polish branch of the American company Bunge. Physicochemical parameters of rapeseed oil were as follows:

- acid number - 0.1 mg KOH/g,
- peroxide number - 0.0 meq of active oxygen per kg,
- water and volatile matter content - 0.02% (m/m),

- content of unsaponifiables in petroleum ether, - 0.01% (m/m),
- content of unsaponifiable matter – 0.8% (m/m)

RME samples were stored at 15 °C in a refrigerator to avoid the influence of external factors on the RME thermophysical properties.

Main components of the measured RME sample are: methyl ester of oleic acid C18:1 (60.7%), methyl ester of linoleic acid C18:2 (19.9%), methyl ester of linolenic acid C18:3 (9.1%) and a vestigial amount of methyl esters of other unsaturated and saturated fatty acids, see Table 1. The chemical composition of the measured RME sample was determined using the gas chromatography Hewlett-Packard HP 6890 device working in conjunction with a Flame Ionization Detector and a high-polar column BPX70. The subsequent analysis was performed following the AOCS Cd 11b-91 methodology according to the ISO 5508 and ISO 5509 standards.

The RME fabricated by the Institute of Agriculture and Food Biotechnology satisfied the specifications of the European Standard for Biodiesel (EN 14214). Analysis of the RME properties compliance with the EN 14214 Standard is summarized in Table 2.

Table 1
Fatty acids composition of the investigated FAME sample according to the ISO standard 5508.

Fatty acid	Amount (%)
C 14:0	0.1
C 16:0	4.5
C 16:1	0.3
C 17:0	0.1
C 17:1	0.1
C 18:0	1.8
C 18:1 cis9	58.1
C 18:1 cis11	2.6
C 18:2 cc	19.9
C 18:3 ccc	9.1
C 20:0	0.6
C 20:1	1.5
C 20:2	0.1
C 22:0	0.3
C 22:1	0.5
C 24:0	0.2
C 24:1	0.2

Table 2
Comparison of the measured parameters of the investigated RME sample with the specifications of the European Standard for Biodiesel (EN 14214).

Property	Unit	Result	Lower limit	Upper limit	Test Method
Ester content	% (m/m)	98.9	96.5	–	EN 14103
Water content	mg/kg	100	–	500	EN ISO 12937
Density at 15 °C	g/cm^3	0.8798	0.86	0.90	EN ISO 3675
Viscosity at 40 °C	mm^2/s	4.37	3.5	5.0	EN ISO 3104
Sulfur content	mg/kg	5	–	10	EN ISO 20846
Methanol content	% (m/m)	0.1	–	0.2	EN 14110
Monoglyceride content	% (m/m)	0.4	–	0.7	EN 14105
Diglyceride content	% (m/m)	0.05	–	0.2	EN 14105
Triglyceride content	% (m/m)	0,05	–	0.2	EN 14105
Free glycerol	% (m/m)	0.02	–	0.02	EN 14105
Total glycerol	% (m/m)	0.10	–	0.25	EN 14105
Alkali content (Na + K)	mg/kg	2	–	5	EN 14108
Phosphorus content	mg/kg	2	–	4	EN 14107
Acid value	mg KOH/g	0.2	–	0.5	EN 14104
Iodine value	–	118	–	120	EN 14111

2.2. High-pressure experimental setup

The original experimental setup for high pressure measurements of liquid properties was developed and constructed by the Authors at Institute of Fundamental Technological Research in Warsaw, Poland [18–22], see Fig. 1. High pressures were obtained in a thick-walled cylindrical chamber with a simple piston and a Bridgman II sealing system. The pressure inside the chamber was measured with an 104 Ω manganin transducer. Its resistance (pressure dependent) was measured by a NI 4065 multimeter PC board provided by National Instruments Corp., USA. The pressure inside the chamber was measured with a 2σ uncertainty of 0.1%.

The temperature inside the chamber was kept constant within $\pm 0.1\ ^{\circ}C$ due to employment of a thermostatic water bath with a precision thermostatic device provided by Julabo Labortechnik, Seelbach, Germany. A type T type copper-constantan thermocouple was placed directly inside the high-pressure chamber, for temperature measurements.

The piezoelectric transducers (bulk and surface wave), were driven by the TB-1000 pulser-receiver PC board, provided by Matec, USA. The signals received by piezoelectric transducers were amplified by the TB-1000 receiver and sent into the PDA-1000 digitizer board, provided by Signatec, USA.

The PC boards were installed inside an industrial PC computer, provided by Transduction, Mississauga, Canada. Whole experimental setup was controlled by a custom software written in the Visual C++ software development environment provided by Microsoft, working in conjunction with the Measurement Studio software package provided by National Instruments.

The viscosity sensor (B-G wave piezoceramic waveguide) was built with a metalized piezoelectric plate with dimensions $6 \times 40 \times 10$ mm (width, length and height). The viscosity sensor (B-G wave piezoceramic waveguide) was placed directly inside the high-pressure chamber. The ultrasonic transducer generating and receiving B-G surface waves was driven by the tone burst TB-1000 pulser-receiver board with a radio frequency of $f = 2\ MHz$ and pulse length $\sim 0.5\ \mu s$. The impulse generated by the B-G wave transducer was multiply reflected between the two opposite edges of the B-G wave waveguide. Thus, the ultrasonic signal received by the transmitting-receiving B-G wave transducer was composed of a train of several consecutive echoes with a diminishing amplitude. It is worth noticing that the B-G surface acoustic waves are shear (transverse) waves propagating in piezoelectric waveguides. Thus, by its nature shear wave waveguides can “sense” the viscosity of the adjacent liquid, since shear stresses in the liquid are, by definition, proportional to the liquid viscosity.

Measurements of the speed of sound c were performed in the same high-pressure chamber, which was used for viscosity measurements. However, in contrast to the viscosity measurements the speed of sound c in liquids was measured using bulk compressional (longitudinal) ultrasonic waves, propagating directly in the measured liquid. Two piezoelectric transducers, first generating and second receiving compressional (longitudinal) ultrasonic waves in the liquid, were placed directly in the high-pressure chamber. The compressional (longitudinal) piezoelectric transducers were facing each other and were in a direct contact with the measured liquid. The compressional (longitudinal) piezoelectric transducers (Y-36 cut $LiNbO_3$) were provided by Boston Piezo-Optics Inc., USA.

2.3. Measurements of the viscosity η

It should be stressed that both types of the surface acoustic waves (Love or B-G waves) used by the Authors are shear horizontal (SH) transverse waves, with direction of particle vibration perpendicular to the direction of wave propagation.

Love or B-G solid waveguides, employed in viscosity measurements in liquids, are immersed directly in the measured liquid. Due to the interaction with the surrounding liquid the B-G wave

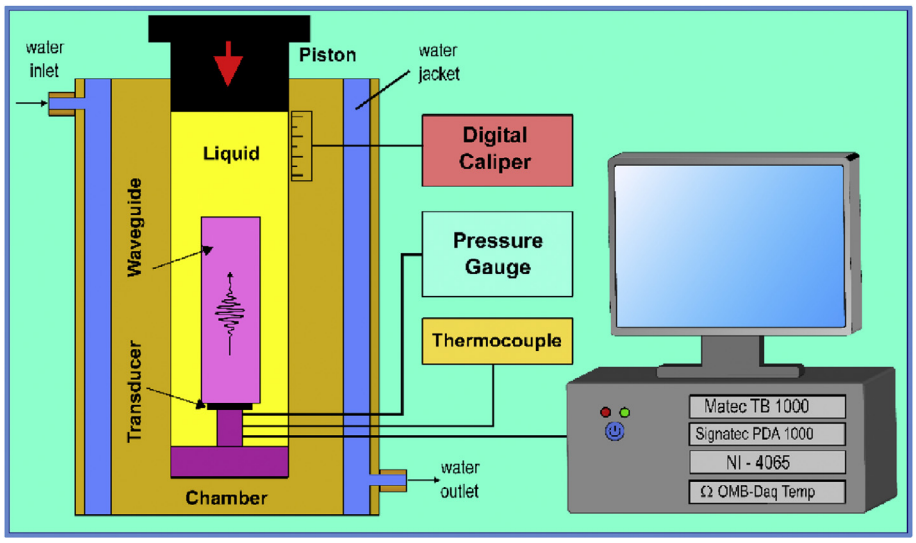

Fig. 1. Computerized ultrasonic experimental setup for measuring the viscosity of biofuels at high pressures and various values of temperature.

changes its velocity and amplitude. The mechanical load exerted by the liquid on the piezoceramic waveguide is proportional to the shear impedance Z_L of the liquid. In general, for sinusoidal waves the impedance Z_L is described by a complex quantity $Z_L = R_L + jX_L$, where $j = (-1)^{1/2}$ is the imaginary unit. The shear mechanical impedance of the liquid Z_L can be determined from measurements of the attenuation and phase of the SAW wave impulses propagating in the solid waveguide loaded by the liquid [23]. The viscosity η of the liquid can be determined from the following formula: $\eta = 2R_L^2/\omega\rho$, where: R_L is the real part of the mechanical shear impedance Z_L of the liquid, ρ is the liquid density, ω the angular frequency of the Love or B-G wave and η the viscosity of the liquid.

2.4. Measurements of the speed of sound c

The ultrasonic waves used to measure the speed of sound c in liquids are bulk compressional (longitudinal) waves, i.e., with the direction of particle vibrations parallel to the direction of propagation of the wave.

The speed of sound c of these compressional pressure waves in the liquid was determined from the following elementary formula: $c = L/TOF$, where L is the distance between two ultrasonic transducers and TOF is the time-of-flight required for the ultrasonic impulses to travel between the transmitting and receiving ultrasonic transducers, in the measured liquid. The time of flight (TOF) between the two consecutive ultrasonic impulses was determined in the controlling PC computer using a cross-correlation method [24–26]. The expanded 2σ uncertainty for the speed of sound c of compressional pressure waves in the liquid was estimated to be 0.3%.

2.5. Measurements of the liquid density ρ

The density ρ of the RME sample was determined from measurements of the sample mass m and its actual volume V, using the standard formula $\rho = m/V$.

In order to determine changes in the density ρ of the investigated liquid, we measured changes in the volume of the liquid sample subjected to high pressures. The volume changes of the liquid sample were determined from the measured displacement of the piston in the pressure chamber using a digital caliper. Initially, the density ρ of the liquid sample was measured at an atmospheric pressure by a Jaulmes pycnometer. The changes in density ρ of the RME sample were measured as a function of pressure p at various constant temperatures T. The standard uncertainty σ for the measurements of density ρ was estimated to be 0.1%.

3. Experimental results

3.1. Speed of sound c measured in RME

Fig. 2 shows the isotherms of the speed of sound c (pressure waves) measured as a function of pressure p at a frequency 5 MHz, and at temperatures T: 5, 10, 15, and 20 °C.

The pressure in the high pressure chamber was applied incrementally with a step of 10 MPa, from an atmospheric pressure up to 250 MPa. Each pressure increase was followed by a time interval of 5 min, allowing the RME sample to achieve the conditions of thermodynamic equilibrium.

To facilitate subsequent calculations, the speed of sound c, measured in the RME sample, was approximated by a polynomial of the order 3 with 2 independent variables i.e., pressure p and temperature T. As a result, the following empirical formula for the speed of sound c in RME has been obtained:

$$c(p,T) = a + bp + cT + dp^2 + eT^2 + fpT + gp^3 + hT^3 + ipT^2 + jp^2T \quad (1)$$

where the coefficients of the polynomial are as follows: a = 1.581806047, b = 0.004172975, c = −0.00623323, d = −5.06e-06, e = 0.000235852, f = −2.5277e-05, g = 1.35455e-08, h = −1.3458e-05, i = 3.56471e-06, j = −2.7979e-07.

To assess the quality of the polynomial approximation with Eq. (1), we compared the values of the speed of sound c measured in the RME sample with the numerical values provided by the polynomial approximation. To quantify the difference between the measured and approximated values of the speed of sound c, we calculated a number of the corresponding statistical parameters, such as the absolute average deviation (AAD), the maximum deviation (MD), the average deviation (Bias) and the standard deviation σ that are defined, respectively, as follows [28].

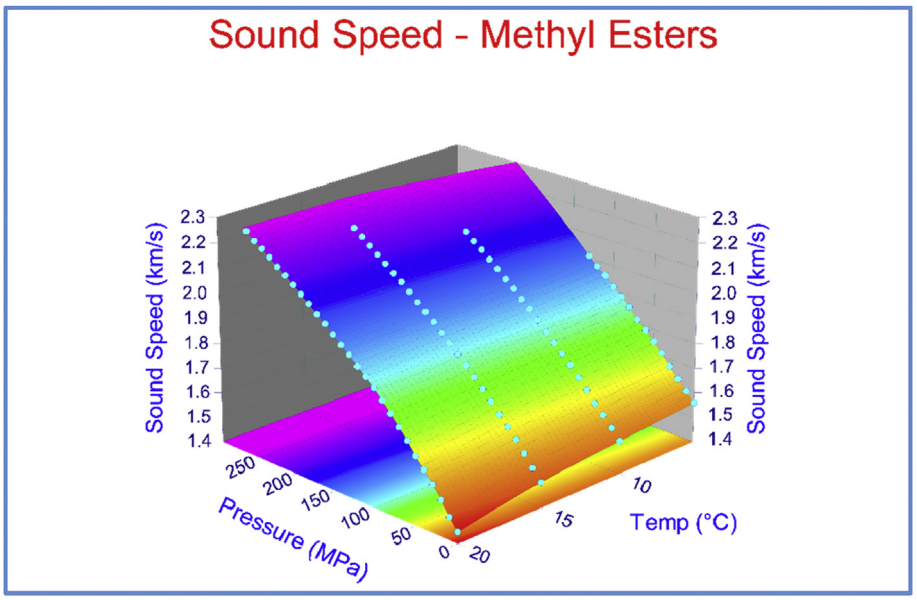

Fig. 2. Speed of sound c (pressure waves) measured in the RME sample versus pressure p and temperature T, for ultrasonic waves at a frequency of $f = 5$ *MHz*.

$$AAD = \frac{100}{N}\sum_{i=1}^{N}\left|\frac{c_i^{exp} - c_i^{cal}}{c_i^{exp}}\right| \tag{2}$$

$$MD = max\left(100\left|\frac{c_i^{exp} - c_i^{cal}}{c_i^{exp}}\right|\right) \tag{3}$$

$$Bias = \frac{100}{N}\sum_{i=1}^{N}\frac{c_i^{exp} - c_i^{cal}}{c_i^{exp}} \tag{4}$$

$$\sigma = \sqrt{\frac{\sum_{i=1}^{N}\left(c_i^{exp} - c_i^{cal}\right)^2}{N-m}} \quad i = 1, \cdots, N \tag{5}$$

where: c_i^{exp} is the experimentally measured speed of sound, c_i^{cal} represents the speed of sound calculated from the polynomial formula (Eq. (1)), N is the number of the experimental data ($N = 86$) and m is the number of adjustable parameters in the polynomial formula (in our case $m = 10$).

Statistical parameters of the polynomial approximation for the measured speed of sound c in the RME sample are given in Table 3.

The approximation given in Eq. (1) was performed with the software package Table Curve 3D (Systat, USA).

3.2. Density ρ measured in RME

Fig. 3 shows the results of measurements for the density ρ of the RME sample versus pressure p and temperature T.

Similarly to the speed of sound c, the measured density ρ of the rapeseed methyl esters was approximated by a fifth order polynomial of two independent variables, p and T, as follows:

$$\rho(p,T) = a_1 + b_1 p + c_1 p^2 + d_1 p^3 + e_1 p^4 + f_1 p^5 + g_1 T + h_1 T^2 + i_1 T^3 \tag{6}$$

where: a = 0.889802845, b = 1.2551e-05, c = 7.16522e-07, d = −6.3172e-09, e = 2.32501e-11, f = −3.1429e-14, g = −0.00040858, h = −3.0012e-05, i = 8.21127e-07.

To evaluate the quality of the approximation with Eq. (6) the statistical parameters given by Eqs. (2)–(6), were calculated and presented in Table 4.

The calculated statistical parameters (AAD, MD, Bias and Standard Deviation) are lower than the experimental uncertainties of the speed of sound c and density ρ. Therefore, the values of the speed of sound c and density ρ, determined from the polynomial approximations (Eqs. (1) and (6)), can be used in the following calculations involving the measured speed of sound c and density ρ of the RME sample.

The approximation given in Eq. (6) was performed with the software package Table Curve 3D (Systat, USA).

Table 3
Statistical parameters of the polynomial approximation (Eq. (1)) for the measured speed of sound c in the RME sample. r^2 is the coefficient of determination.

Statistical parameter	AAD (%)	MD (%)	Bias (%)	σ (m/s)	r^2
Numerical value	0.10	0.38	−0.00017	2.5	0.9998

3.3. Viscosity η measured in RME

The viscosity η of the investigated RME sample at an atmospheric pressure was measured with an Ubbelohde type capillary viscometer, see Table 5.

The viscosity η of the RME sample was subsequently measured as a function of pressure p (from atmospheric up to 350 MPa, step 10 MPa) for different temperatures T (from 5 °C to 20 °C), using the original ultrasonic B-G waves method developed by the authors [16–18]. The results of measurements for the viscosity η are presented in Fig. 4.

The viscosity η of the RME sample (see Fig. 4) displays three significantly different characteristics. Namely, a low-pressure phase region (blue color), a phase transition region (black color), and a high-pressure phase region (red color).

Initially the pressure was gradually increased from an atmospheric pressure until a first-order phase transition began (blue

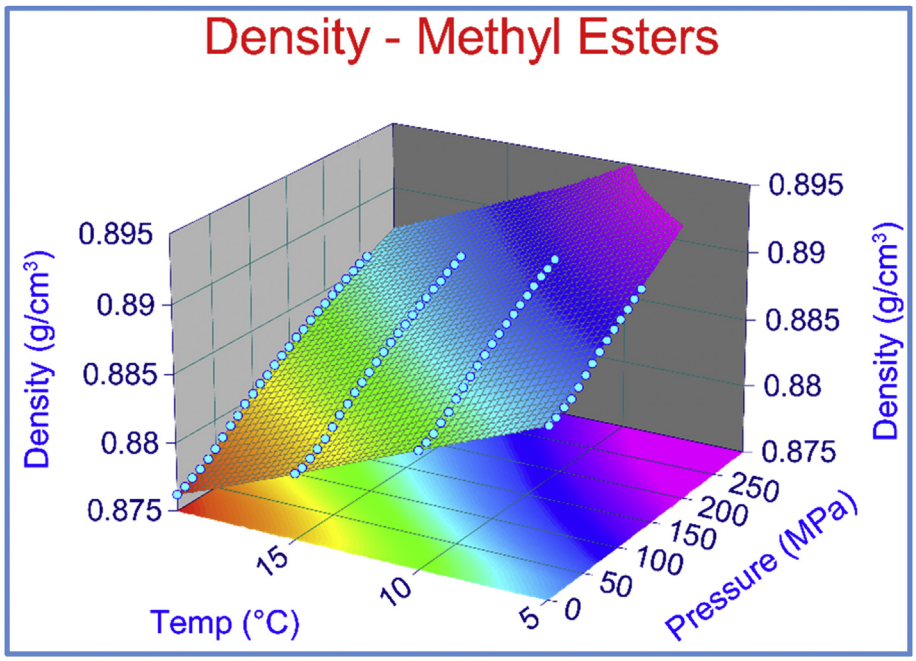

Fig. 3. Density ρ of the RME sample measured as a function of pressure p and temperature T.

Table 4
Statistical parameters of the polynomial approximation (Eq. (6)) for the measured density ρ of the RME sample. r^2 is the coefficient of determination.

Statistical parameter	AAD (%)	MD (%)	Bias (%)	σ (g/cm^3)	r^2
Numerical value	0.00475	0.015	-4.82×10^{-7}	6.9×10^{-5}	0.9998

Table 5
Viscosity η of the RME sample measured at atmospheric pressure.

Temperature (°C)	5	10	15	20
Viscosity η (mPas)	9.426	8.012	6.928	6.042

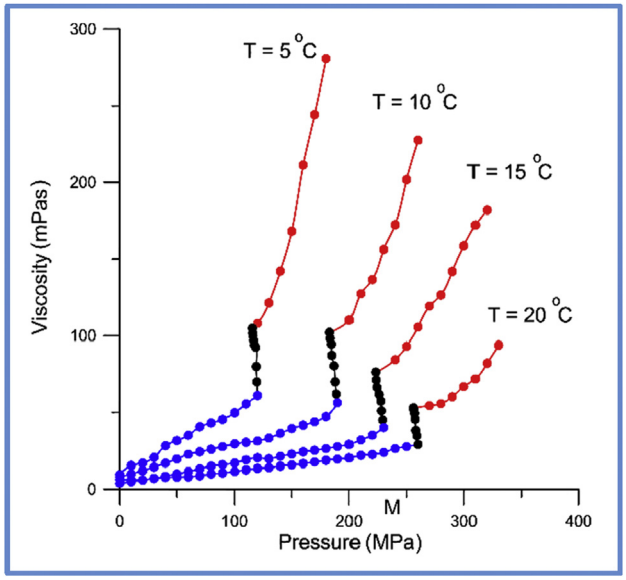

Fig. 4. Viscosity η of the rapeseed methyl esters sample measured as a function of pressure p for different temperatures ($T = 5\,^{\circ}C, 10\,^{\circ}C, 15\,^{\circ}C$ *and* $20\,^{\circ}C$).

part of each curve in Fig. 4). The viscosity in this region was increasing almost exponentially according to the empirical Barus formula. Subsequently, we observed a spontaneous pressure drop in the pressure chamber, which indicates initiation of the phase transition process (black part of each curve in Fig. 4). When the phase transition was completed, the resulting high-pressure phase was further compressed (red part in each curve in Fig. 4).

Phase transition (solidification) regions are clearly visible in Fig. 4, see black part in curves in Fig. 4. When we detected a phase transition, e.g., at 190 MPa for a temperature of 10 °C, we stopped immediately the compression of the sample and the piston in the high-pressure chamber was immobilized in a fixed position in order to enable the phase transition to occur in quasi-static conditions. During the phase transition, the viscosity of the liquid shows a spontaneous and rapid raise despite the pressure drop. At the end of the phase transition process we started to increase the pressure again (see high-pressure phase parts marked red in Fig. 4). When the temperature during measurements was higher, the pressure, at which the phase transition started, increased (e.g. 130 MPa for 5 °C and 260 MPa for 20 °C). Consequently, the pressure at which transition stopped was also higher. The stabilization of pressure and negligible changes in viscosity indicate that the high-pressure phase transition is completed.

4. Phase transitions in RME

The presence of the high-pressure phase transitions in biofuels is a highly undesirable effect, since it can result in a damage of the diesel engine and its fuel injection systems.

It is noteworthy that phase transitions in RME, at high pressures, were investigated previously using an optical method [8]. However, the optical method employed gives only qualitative results, since only the presence or absence of a high-pressure phase transition can be detected. Changes in physicochemical parameters of the liquids (e.g., viscosity) during the phase transitions cannot be quantified with the reported optical method.

The high-pressure phase transitions, which were observed in

the investigated RME sample are high-pressure phase transitions of the first order. This is due to the following phenomena, which were observed during phase transitions in the examined RME sample:

1) a change in the volume of the RME sample
2) a discontinuous and rapid change in the viscosity η of the RME sample
3) a spontaneous pressure drop
4) an abrupt change of the density ρ of the RME sample

Similar high-pressure phase transitions were discovered by the Authors in other liquids (oils), i.e., in the triacylglycerol (TAG), diacylglycerol (DAG), oleic acid, castor oil and olive oil [19,23–25,27], using SH (Shear Horizontal) ultrasonic surface waves of the B-G and Love type, propagating in solid waveguides. Nevertheless, the high-pressure phase transitions in the examined RME (FAME) are still not well understood and require further research.

5. Thermophysical parameters of the RME evaluated from the measured speed of sound *c* and density ρ

All thermophysical parameters of RME presented in this section, such as bulk modulus B, and surface tension σ, were calculated in the low-pressure phase region, i.e., for pressures lower than 250 MPa.

5.1. Bulk modulus B

The bulk modulus B is a crucial parameter that characterizes the behavior of fuels in the injection systems in diesel engines [29]. The adiabatic bulk modulus B (at a constant entropy S) was determined from the following expression [30]:

$$B(p,T) = \frac{1}{\beta_s(p,T)} = \rho(p,T)\left(\frac{\partial p}{\partial \rho}\right)_S = \rho(p,T)\, c^2(p,T) \quad (Pa) \qquad (7)$$

where: β_s is the adiabatic compressibility, ρ is the density measured in the RME sample and c is the speed of sound measured in the RME sample.

Dependence of the bulk modulus B in the RME sample, on pressure p and temperature T, evaluated from Eqs. (1), (6) and (7) is presented in Fig. 5.

5.2. Surface tension σ

Surface tension is one of the key parameters of biofuels that directly affects fuel atomization. For example, a large value of the surface tension makes the formation of small droplets difficult, hindering the correct fuel atomization in the engine combustion chamber [31,32]. The surface tension σ is defined as the energy dW (Gibbs free energy) that must be supplied to increase the surface area of a liquid by one unit dA, namely [31,33].

$$\sigma(p,T) = \frac{dW}{dA} = 6.33\cdot 10^{-10}\cdot \rho(p,T)\cdot c(p,T)^{3/2} \quad \left(\frac{N}{m}\right) \qquad (8)$$

Fig. 6 displays the dependence of the surface tension σ in the RME sample versus pressure p and temperature T, computed from Eqs. (1), (6) and (8).

Measurements of the viscosity η and other thermophysical properties of biofuels at high pressures is of paramount importance in determination of the exploitation properties of biofuels used in diesel engines. For example, knowledge of the fuel viscosity η, surface tension σ, density ρ and bulk modulus B is of crucial importance in modeling and optimization of the atomization process in injection systems, e.g., common rail, and biofuels

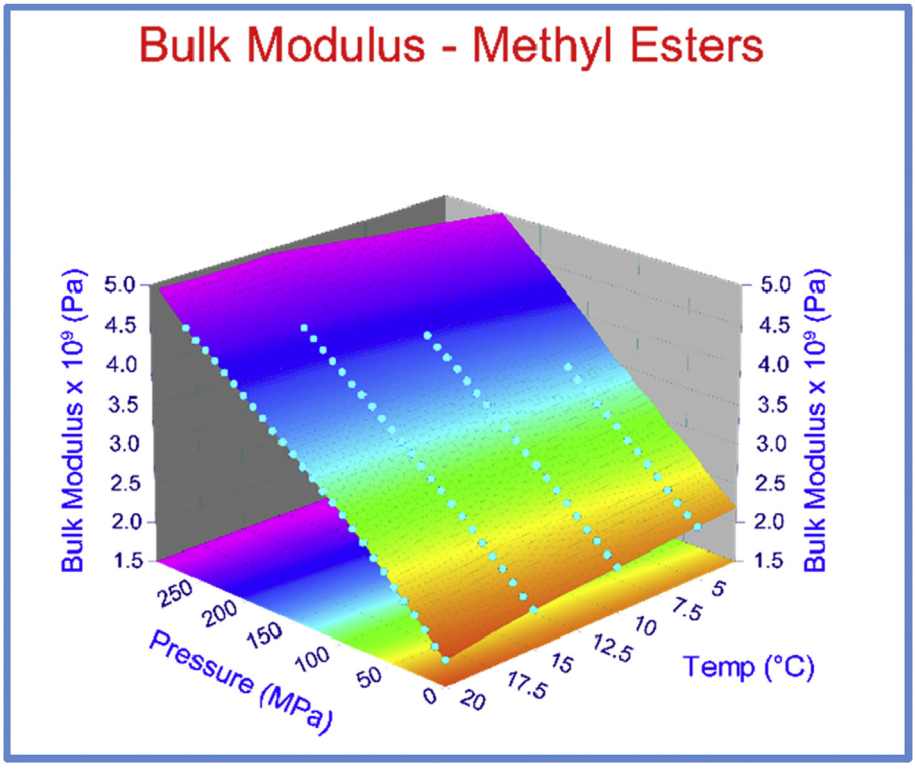

Fig. 5. Bulk modulus B of the RME sample as a function of pressure p and temperature T.

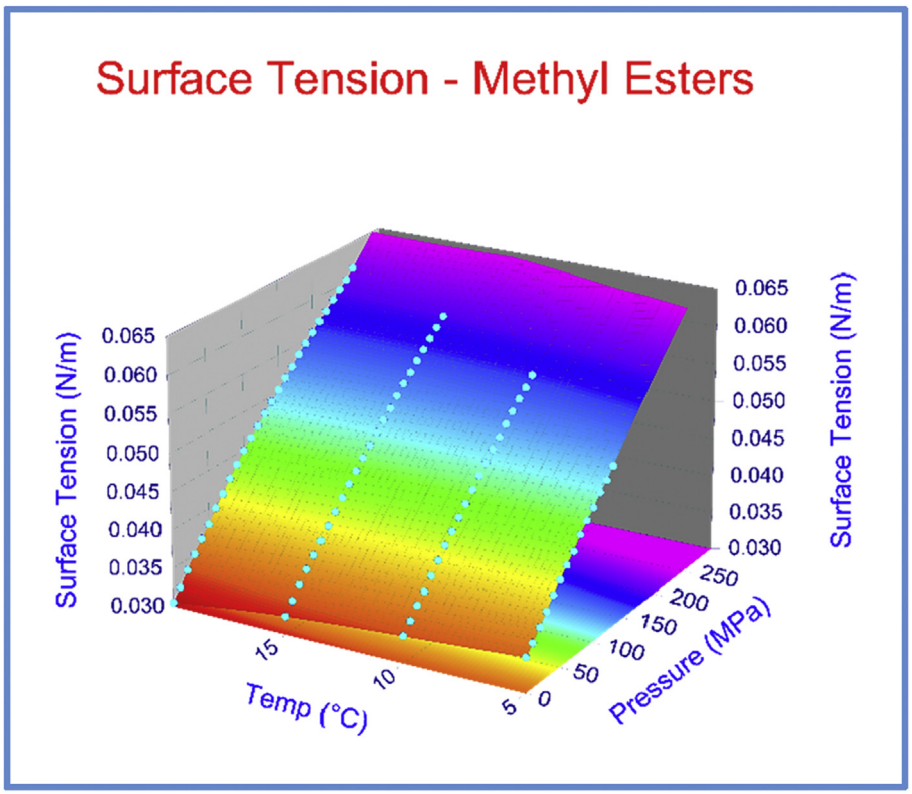

Fig. 6. Variation of the surface tension σ of the RME sample on pressure p and temperature T.

combustion dynamics [34–42].

Measurements of the viscosity η in the RME sample, performed with the B-G waves ultrasonic method, in a wide range of pressures, revealed the existence of the first order high-pressure phase transitions at pressures above 100 MPa, see Fig. 4. These measurements also enabled for the determination of the values of pressures at which the phase transitions initiate and terminate.

During the phase transition the hydrostatic pressure slightly decreases, while the value of the viscosity η raises significantly. For example, at a temperature of 10 °C, the viscosity η raises from 56 mPas to 102 mPas at a pressure of ~180 MPa, see Fig. 4. With an increasing temperature (see Fig. 4), the pressure at which the phase transition begins is higher. For example, at a temperature of 5 °C the phase transition occurs at ~130 MPa, whereas at a temperature of 20 °C at ~260 MPa. With decreasing temperatures, the phase transition is completed faster. For example, at temperatures 20, 15, 10 and 5 °C the phase transition was completed, in about 8, 6, 4 and 3 min, respectively.

The discontinuous change in the viscosity η of the RME sample as a function of pressure is a strong evidence that the first order high-pressure phase transition occurs in the investigated RME sample.

At higher temperatures, these phase transitions (solidification) may occur at higher pressure values. Based on the results of the research conducted by the authors, it can be estimated that the high pressure phase transition in RME at temperature $t = 30\,°C$ is expected at $p = 350\,MPa$. Similarly, for $t = 40\,°C$ this high-pressure phase transition is expected at $p = 450\,MPa$. These pressure values are above the pressure range that is employed in contemporary injection systems (e.g., common rail).

Fig. 5 shows that the bulk modulus B of the RME sample grows with increasing pressures, and decreases with increasing temperatures.

As illustrated in Fig. 6, the surface tension σ of the RME sample diminishes with the raise of temperature, and increases with the growing pressure, as one might expect.

6. Conclusions

The main implications resulting from this work can be summarized as follows:

1) Knowledge of quantitative and qualitative characteristics of high-pressure phase transitions and high-pressure behavior of thermophysical parameters of biofuels is of crucial importance for engineers and designers of modern fuel injection systems of the common rail type for diesel engines.
2) Ultrasonic methods (speed of sound and density measurements) allow for relatively simple evaluation of many key high-pressure thermophysical parameters of biofuels, e.g., surface tension and bulk modulus.
3) Innovative B-G waves ultrasonic technique has been used successfully in detection and quantification of high-pressure (200 MPa) first order phase transitions (solidification) occurring in the RME material being a biofuel component.
4) The change in the viscosity of RME (in contrary to changes in the speed of sound and density of RME) is very clear and precise indicator of phase transitions occurring in RME. In fact, during the phase transition in RME, the speed of sound c changes approximately only 0.3%. By contrast, the changes in the viscosity η of RME during the high-pressure phase transition were of the order of 100%.
5) The discovered high-pressure phase in RME, occurring after the phase transition (solidification), is characterized by high viscosity, what can be very detrimental for the performance of modern fuel injection systems of the common rail type, where

pressures above 200 MPa, kept an extended period of time, are common, especially under cold-start conditions.

The precise knowledge of the high-pressure thermophysical parameters of biofuels, is of vital importance in the design and optimization of modern fuel injection systems (common rail) in diesel engines. Namely, the thermophysical parameters of the fuel directly affect the pressure wave amplitude and consequently the mass flow rate and the total amount of the fuel injected in the cylinder.

Density is the main parameter that influences the conversion of the fuel volume flow rate q_V into mass flow rate q_m, here the following relation holds: $q_m = \rho \cdot q_V$. The bulk modulus affects the fuel pressure wave amplitude and also its velocity and consequently the fuel injection timing. The viscosity of the fuel impacts the pressure wave damping and the pressure loss in the injector feed pipe. Surface tension along with viscosity, density and bulk modulus determine the quality of atomization of biofuels in diesel engines.

For this reason, a complete (precise) knowledge of thermophysical parameters of fuel (such as viscosity, bulk modulus, density and surface tension) in a high-pressure range is of great importance for practitioners, engineers and designers of fuel injection systems in diesel engines of the common rail type to establish a mathematical model of diesel engine operation.

References

[1] E.H.I. Ndiaye, J.P. Bazile, D. Nasri, C. Boned, J.L. Daridon, High pressure thermophysical characterization of fuel used for testing and calibrating diesel injection systems, Fuel 98 (2012) 288–294.
[2] A. Demirbas, Biodiesel. A Realistic Fuel Alternative for Diesel Engines, Springer, London, 2008.
[3] G. Knothe, J. Van Gerpen, J. Krahl (Eds.), The Biodiesel Handbook, AOCS Press, Champaign, Illinois, 2005.
[4] F.A. Uriarte Jr., Biofuels from Plant Oils, ASEAN Foundation, Jakarta, 2010.
[5] G. Knothe, L.F. Razon, Biodiesel fuels, Prog. Energy Combust. Sci. 58 (2017) 36–59.
[6] S.K. Hoekman, A. Broch, C. Robbins, E. Ceniceros, M. Natarajan, Review of biodiesel composition, properties, and specifications, Renew. Sustain. Energy Rev. 16 (2012) 143–169.
[7] J. Merkisz, P. Fuć, P. Lijewski, M. Kozak, Rapeseed oil methyl esters (RME) as fuel for urban transport, in: K. Biernat (Ed.), Alternative Fuels, Technical and Environmental Conditions, Intechopen, Rijeka, 2016 (Chapter 2).
[8] R. Tarakowski, A. Malanowski, A.J. Rostocki, M. Kowalczyk, P. Modzelewski, S. Ptasznik, R.M. Siegoczynski, Could RME biodiesel be potentially harmful to modern engine? Solidif. Process RME, Fuel 146 (2015) 28–32.
[9] P.A. Giuliano Albo, S. Lago, H. Wolf, R. Pagel, N. Glen, M. Clerck, P. Ballereau, Density, viscosity and specific heat capacity of diesel blends with rapeseed and soybean oil methyl ester, Biomass Bioenergy 96 (2017) 87–95.
[10] J. Galle, S. Defruyt, C. Van de Maele, R. Piloto Rodriguez, Q. Denon, A. Verliefde, S. Verhelst, Experimental investigation concerning the influence of fuel type and properties on the injection and atomization of liquid biofuels in an optical combustion chamber, Biomass Bioenergy 57 (2013) 215–228.
[11] C.E. Ejim, B.A. Fleck, A. Amirfazli, Analytical study for atomization of biodiesels and their blends in a typical injector: surface tension and viscosity effects, Fuel 86 (2007) 1534–1544.
[12] A.M. Duncan, A. Ahosseini, R. McHenry, C.D. Depcik, S.M. Stagg-Williams, A.M. Scurto, High-pressure viscosity of biodiesel from soybean, Canola, and Coconut oils, Energy Fuels 24 (2010) 5708–5716.
[13] M.J. Pratas, S.V.D. Freitas, M.B. Oliveira, S.C. Monteiro, A.S. Lima, J.A.P. Coutinho, Biodiesel density: experimental measurements and prediction models, Energy Fuels 25 (2011) 2333–2340.
[14] C. Aparicio, B. Guignon, L.M. Rodriguez-Anton, P.D. Sanz, Determination of rapeseed methyl ester oil volumetric properties in high pressure (0.1 to 350 MPa), J. Therm. Analysis Calorim. 89 (2007) 13–19.
[15] M.J.W. Povey, Applications of ultrasonics in food science - novel control of fat crystallization and structuring, Curr. Opin. Colloid Interface Sci. 28 (2017) 1–6.
[16] P. Kiełczyński, W. Pajewski, M. Szalewski, A. Balcerzak, Measurement of the shear storage modulus and viscosity of liquids using the Bleustein–Gulyaev wave, Rev. Sci. Instrum. 75 (2004) 2362–2367.
[17] P. Kiełczyński, M. Szalewski, R.M. Siegoczyński, A.J. Rostocki, New ultrasonic Bleustein-Gulyaev wave method for measuring the viscosity of liquids at high pressure, Rev. Sci. Instrum. 79 (2008), 026109–1-3.
[18] A.J. Rostocki, R.M. Siegoczyński, P. Kiełczyński, M. Szalewski, An application of Love SH waves for the viscosity measurement of triglycerides at high pressures, High Press. Res. 30 (2010) 88–92.
[19] P. Kiełczyński, M. Szalewski, A. Balcerzak, A.J. Rostocki, D.B. Tefelski, Applications of SH surface acoustic waves for measuring the viscosity of liquids in function of pressure and temperature, Ultrasonics 51 (2011) 921–924.
[20] P. Kiełczyński, M. Szalewski, A. Balcerzak, A. Malanowski, R.M. Siegoczyński, S. Ptasznik, Investigation of high-pressure phase transition in DAG (diacylglycerol) oil using the Bleustein-Gulyaev ultrasonic wave method, Food Res. Int. 49 (2012) 60–64.
[21] P. Kiełczyński, M. Szalewski, A. Balcerzak, K. Wieja, A. Malanowski, R. Kościesza, R. Tarakowski, A.J. Rostocki, R.M. Siegoczyński, Determination of physicochemical properties of diacylglycerol oil at high pressure by means of ultrasonic methods, Ultrasonics 54 (2014) 2134–2140.
[22] P. Kiełczyński, M. Szalewski, A. Balcerzak, K. Wieja, A.J. Rostocki, R.M. Siegoczyński, Ultrasonic evaluation of thermodynamic parameters of liquids under high pressure, IEEE Trans. Ultrason. Ferroelectr. Freq. Contr. 62 (2015) 1122–1131.
[23] P. Kiełczyński, Application of acoustic waves to investigate the physical properties of liquids at high pressure, in: D. Dissanayake (Ed.), Acoustic Waves, Sciyo, Rijeka, 2010, pp. 317–340 (Chapter 14).
[24] A.J. Rostocki, R.M. Siegoczyński, P. Kiełczyński, M. Szalewski, A. Balcerzak, M. Zduniak, Employment of a novel ultrasonic method to investigate high pressure phase transitions in oleic acid, High Press. Res. 31 (2011) 334–338.
[25] A.J. Rostocki, R. Tarakowski, P. Kiełczyński, M. Szalewski, A. Balcerzak, S. Ptasznik, The ultrasonic investigation of phase transition in olive oil up to 0.7 GPa, J. Am. Oil Chemists' Soc. 90 (2013) 813–818.
[26] P. Kiełczyński, M. Szalewski, A. Balcerzak, K. Wieja, A.J. Rostocki, R.M. Siegoczyński, S. Ptasznik, Application of ultrasonic wave celerity measurement for evaluation of physicochemical properties of olive oil at high pressure and various temperatures, LWT-Food Sci. Technol. 57 (2014) 253–259.
[27] M. Zulkurnain, F. Maleky, V.M. Balasubramaniam, High pressure processing effects on lipids thermophysical properties and crystallization kinetics, Food Eng. Rev. 8 (2016) 393–413.
[28] M.J.P. Comuñas, J.P. Bazile, A. Baylaucq, C. Boned, Density of diethyl adipate using a new vibrating tube densimeter from (293.15 to 403.15) K and up to 140 MPa. Calibration and measurements, J. Chem. Eng. Data 53 (2008) 986–994.
[29] B.D. Nikolic, B. Kegl, S.D. Markovic, M.S. Mitrovic, Determining the speed of sound, density, and bulk modulus of rapeseed oil, biodiesel and diesel fuel, Therm. Sci. 16 (2007) 505–514.
[30] M.E. Tat, J.H. Van Gerpen, S. Soylu, M. Canakci, A. Monyem, S. Wormley, The speed of sound and isentropic bulk modulus of biodiesel at 21 C from atmospheric pressure to 35 MPa, J. Am. Oil Chemists' Soc. 77 (3) (2000) 285–289.
[31] S.V.D. Freitas, M.B. Oliveira, A.J. Queimada, M.J. Pratas, A.S. Lima, J.A.P. Coutinho, Measurement and prediction of biodiesel surface tensions, Energy Fuels 25 (2011) 4811–4817.
[32] L.F. Ramirez-Verduzco, Models for predicting the surface tension of biodiesel and methyl esters, Renew. Sustain. Energy Rev. 41 (2015) 202–216.
[33] R. Auerbach, Oberflachenspannung und Schallgeschwindigkeit, Experientia 4 (1948) 143–144.
[34] A.C. Koukakou, K. Le Mapihan, J. Pauly, Solid-liquid equilibria under high pressure of pure fatty acid methyl esters, Fuel 109 (2013) 297–302.
[35] H.K. Suh, C.S. Lee, A review on atomization and exhaust emission of a biodiesel-fueled compression ignition engine, Renew. Sustain. Energy Rev. 58 (2016) 1601–1620.
[36] A. Gopinath, S. Puhan, G. Nagarajan, Effect of unsaturated fatty acid esters of biodiesel fuels on combustion, performance and emission characteristics of a DI diesel engine, Int. J. Energy Environ. 1 (2010) 411–430.
[37] F. Boudy, P. Seers, Impact of physical properties of biodiesel on the injection process in a common-rail direct injection system, Energy Convers. Manag. 50 (2009), 2905–2012.
[38] S.V.D. Freitas, J.J. Segovia, M.C. Martin, J. Zambrano, M.B. Oliveira, A.S. Lima, J.A.P. Coutinho, Measurement and prediction of high-pressure viscosities of biodiesel fuels, Fuel 122 (2014) 223–228.
[39] M.J. Pratas, S. Freitas, M.B. Oliveira, S.C. Monteiro, A.S. Lima, J.A.P. Coutinho, Densities and viscosities of fatty acid methyl and ethyl esters, J. Chem. Eng. Data 55 (2010) 3983–3990.
[40] S. Phankosol, K. Sudaprasert, S. Lilitchan, K. Aryusuk, K. Krisnangkura, An empirical equation for estimation of kinematic viscosity of fatty acid methyl esters and biodiesel, J. Am. Oil Chemists' Soc. 92 (2015) 1051–1061.
[41] D. Deshmukh, A. Madan Mohan, T.N.C. Anand, R.V. Ravikrishna, Spray characterization of straight vegetable oils at high injection pressures, Fuel 97 (2012) 879–883.
[42] A.L. Boehman, D. Morris, J. Szybist, The impact of the bulk modulus of diesel fuels on fuel injection timing, Energy Fuels 18 (2004) 1877–1882.